

Supporting Information

**Synergistic nucleation regulation strategy of 4',4''-Tris(carbazol-9-yl)-
triphenylamine and moisture for stably air-processed high-performance
perovskite photodetectors**

*Guo He,^{ab} Dezhi Yang,^{*ad} Sizhe Tao,^a Liqing Yang,^a Dechao Guo,^a Jingbo Zheng,^a Ji
Li,^a Jiangshan Chen^{ad} and Dongge Ma^{*acde}*

Table of contents

1. The molecular structure of TCTA
2. The changes over time in transparency of TCTA-containing PbX_2 precursor after air exposure
3. The XRD spectra of solvent-coordinated adduct powder obtained from PbX_2 solutions without and with air exposure
4. The XRD spectra of the air-processed perovskite films with and without TCTA
5. J - V characteristics of the hole-only devices under dark conditions
6. The responsivities of PPDs with and without TCTA
7. The noise currents and detectivities of PPDs with and without TCTA
8. The fitting data of the TRPL measurements of perovskite with and without TCTA
9. The average dark current densities of the PPDs with and without TCTA.
10. The average peak EQE s of the PPDs with and without TCTA.

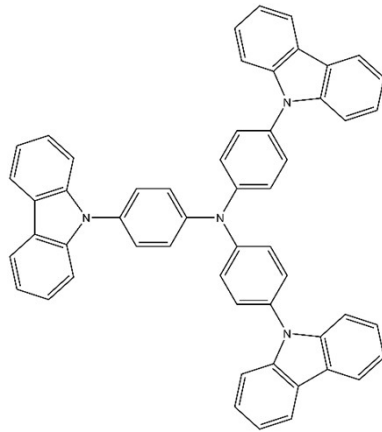


Figure S1. The molecular structure of TCTA

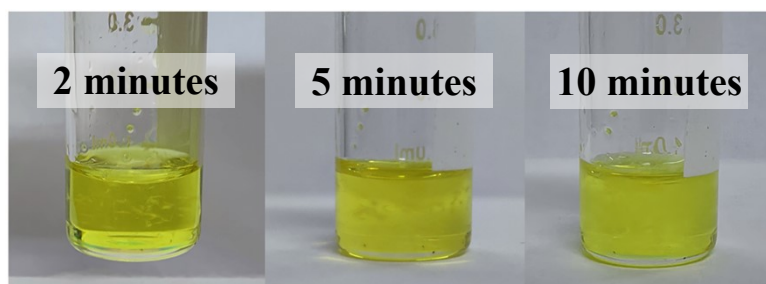


Figure S2. The changes over time in transparency of TCTA-containing PbX_2 precursor after air exposure.

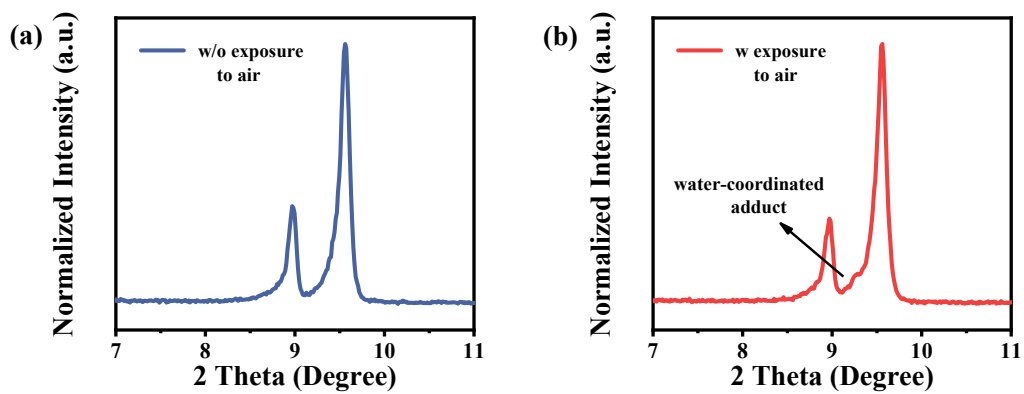


Figure S3. The XRD spectra of solvent-coordinated adduct powder obtained from PbX_2 solutions (a) without and (b) with air exposure.

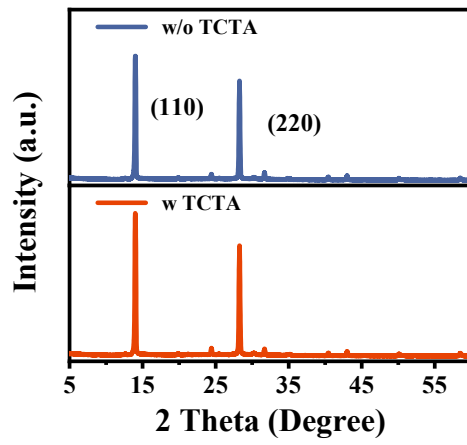


Figure S4. The XRD spectra of the air-processed perovskite films with and without TCTA.

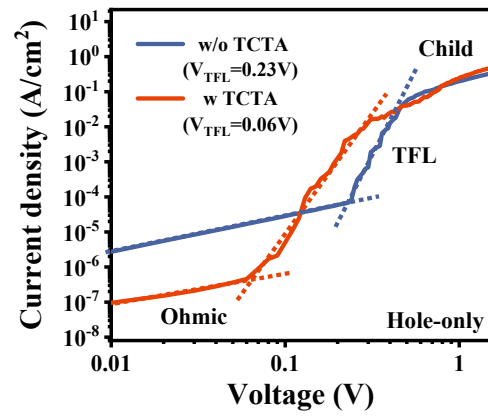


Figure S5. J - V characteristics of the hole-only devices under dark conditions.

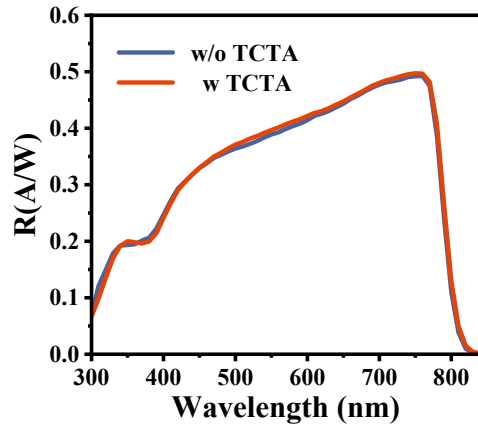


Figure S6. The responsivities of PPDs with and without TCTA.

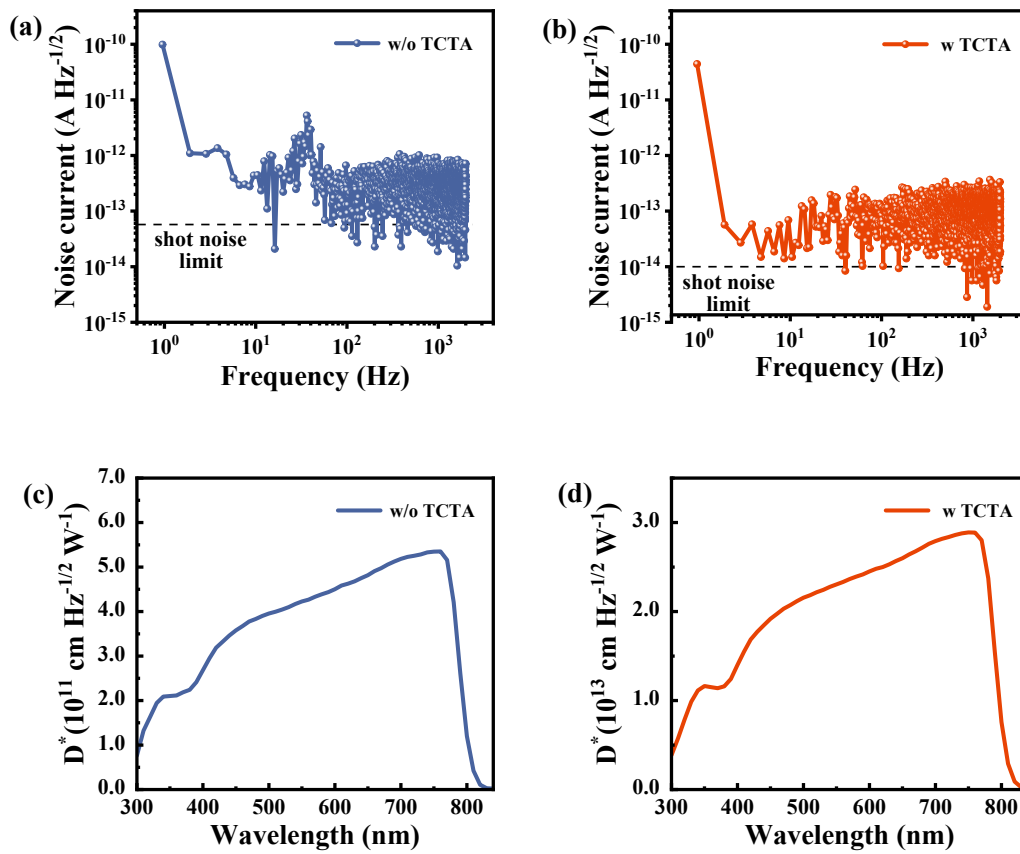


Figure S7. The noise currents and detectivities of PPDs with and without TCTA.

Table S1. The fitting data of the TRPL measurements of perovskite with and without TCTA.

Sample	A_1	τ_1 (ns)	A_2	τ_2 (ns)
W TCTA	157.6	101.2	766.1	382.4
W/o TCTA	533.0	2.7	443.0	10.4

The PL decay curves were fitted using a bi-exponential decay equation :

$$y = A_1 \exp(-x/\tau_1) + A_2 \exp(-x/\tau_2) + y_0$$

Where τ_1 and τ_2 are the lifetimes for the fast and slow components, respectively.

The τ_{ave} is given by the formula:

$$\tau_{\text{ave}} = (A_1 \tau_1^2 + A_2 \tau_2^2) / (A_1 \tau_1 + A_2 \tau_2)$$

Table S2. The dark current densities of the PPDs with and without TCTA.

W	Device number	A1	A2	A3	A4	A5
	J_d (A cm⁻²)	2.2×10^{-10}	3.6×10^{-10}	1.8×10^{-10}	1.1×10^{-9}	2.4×10^{-10}
TCTA	Device number	A6	A7	A8	A9	A10
	J_d (A cm⁻²)	4.7×10^{-10}	7.5×10^{-10}	9.4×10^{-10}	1.0×10^{-9}	2.4×10^{-10}
W/o	Device number	B1	B2	B3	B4	B5
	J_d (A cm⁻²)	3.1×10^{-8}	1.0×10^{-8}	2.2×10^{-8}	2.5×10^{-9}	7.5×10^{-9}
TCTA	Device number	B6	B7	B8	B9	B10
	J_d (A cm⁻²)	4.7×10^{-9}	1.1×10^{-8}	8.3×10^{-9}	4.9×10^{-9}	3.5×10^{-9}

The average dark current densities of PPDs with and without TCTA are 5.6×10^{-10} A cm⁻² and 1.1×10^{-8} A cm⁻², respectively.

Table S3. The peak *EQE*s of the PPDs with and without TCTA.

W	Device number	A1	A2	A3	A4	A5
	<i>EQE</i> (%)	90.1	90.0	96.5	91.9	92.0
TCTA	Device number	A6	A7	A8	A9	A10
	<i>EQE</i> (%)	93.4	91.3	92.44	93.4	93.2
W/o	Device number	B1	B2	B3	B4	B5
	<i>EQE</i> (%)	91.5	92.1	91.3	93.7	90.3
TCTA	Device number	B6	B7	B8	B9	B10
	<i>EQE</i> (%)	90.3	89.4	90.1	91.0	88.6

The average peak *EQE*s of PPDs with and without TCTA are 92.8 % and 90.8 %, respectively.